

GLARE: A Dataset for Traffic Sign Detection in Sun Glare

Nicholas Gray^{*¶}, Megan Moraes^{*¶}, Jiang Bian^{*¶‡}, Allen Tian^{*§}, Alex Wang^{*§}, Haoyi Xiong[†], Zhishan Guo^{¶†}
[¶]University of Central Florida, [‡]Baidu Research Lab, [§]Local High Schools, [†]NC State University

Abstract—Real-time machine learning detection algorithms are often found within autonomous vehicle technology and depend on quality datasets. It is essential that these algorithms work correctly in everyday conditions as well as under strong sun glare. Reports indicate glare is one of the two most prominent environment related reasons for crashes. However, existing datasets, such as LISA and the German Traffic Sign Recognition Benchmark, do not reflect the existence of sun glare at all. This paper presents the GLARE traffic sign dataset: a collection of images with U.S based traffic signs under heavy visual interference by sunlight. GLARE contains 2,157 images of traffic signs with sun glare, pulled from 33 videos of dashcam footage of roads in the United States. It provides an essential enrichment to the widely used LISA Traffic Sign dataset. Our experimental study shows that although several state-of-the-art baseline methods demonstrate superior performance when trained and tested against traffic sign datasets without sun glare, they greatly suffer when tested against GLARE (e.g., ranging from 9% to 21% mean mAP, which are significantly lower than the performances on LISA dataset). We also notice that current architectures have better detection accuracy (e.g., on average 42% mean mAP gain for mainstream algorithms) when trained on images of traffic signs in sun glare.

I. INTRODUCTION

Driving has seen its numerous phases of evolution, from being steam-propelled to becoming almost fully autonomous. Throughout these developments, the existence of one phenomenon has remained constant in the daily environment — intense sunlight which can obstruct the view of a vision sensor (either eyes or cameras) while maneuvering a vehicle. When the sun descends on the horizon, sun glare seeps below a car’s visor and visually impairs vision sensors, causing difficulty in navigating everyday traffic. The temporary blindness (due to sun glare) causes difficulty in sensing other cars, traffic signs, and often leads to accidents. As a result of sun glare, a recent report [1] by the Department of Transportation has stated that as many as 9,000 glare-related accidents occur each year, making it one of the two most prominent environment related reasons for crashes. The combination of harsh sun glare with common driving risk factors contributes to more crashes and congestion in day-to-day driving, leading to setbacks within implementing new automotive technologies.

There has been an upsurge of autonomous vehicles driving alongside everyday drivers, such as Tesla or Google’s Waymo. These self-driving vehicles make their decisions through the use of object detection and classification algorithms, which allows the autonomous system to “see” objects (such as traffic signs on the road), classify them, and make a real-time decision (machine learning [2]) based on the algorithmic interpretation

of the seen object. The functionality of these algorithms heavily depends on rich sets of data that are collected from real-world scenarios, annotated, and fed to “teach” algorithms on what it may experience on the road. One set of data frequently used to teach algorithms within autonomous cars includes traffic signs—critical for navigating everyday traffic. While there are several datasets publicly available that focus on traffic signs in regular weather conditions, there is *few traffic sign dataset focusing on traffic signs with sun glare*. Our experiments indicate that when vehicles are continuously trained to recognize objects using data without sun glare, real-time algorithms within cars may fail to detect traffic signs and other objects when blinded by high-intensity visual noise, leading to catastrophe.

Datasets containing traffic signs with sun glare are often internal within autonomous driving companies and consequently are not publicly available for wider research purposes. While existing public datasets (such as LISA) do not contain any sun glare at all, there is an emerging need to create a public dataset with a wide variety of traffic signs with sun glare interference to fill this disparity.

Contributions. As an addition to the LISA Traffic Sign dataset, we establish the GLARE dataset — a collection of images with traffic signs which have heavy visual interference as a result of strong sunlight. GLARE will be a publicly available set of images for training real-time detection algorithms and more. This dataset and the proposed algorithms are intended to act as a baseline for upcoming researchers while developing, training, and examining their own models. The contributions of this work come in three folds:

- We establish a fine-grained traffic sign dataset, GLARE, with abundant of realistic glares on or near the traffic sign areas. To our knowledge, GLARE is the first traffic sign dataset with detailed annotations of glares and covering a rich scenarios of glare conditions from daily driving. Compared to the common used dataset (e.g., LISA [6], GTSDDB [5], and TT-100K [7]), GLARE provides pure observation of traffic sign with glares instead mixing the sparse witness of general occlusions. We follow the standard format to annotate, calibrate, and reorganize the dataset for a wide range of research tasks (e.g., traffic sign detection, image classification and temporal localization).
- We also have released the full procedures to step-by-step create the dataset and analyze its statistical features.
- We further showcase the research potentials of the GLARE dataset by testing it on a large group of benchmarks. Specifically, we observe that the performances of mainstream traffic sign detection algorithms degrades drastically on GLARE test set, where training with GLARE dataset shows a significant performance gain instead.

* The first five authors contributed equally to this work.

† The corresponding author, zguo32@ncsu.edu.

Work supported in part by NSF Grants CNS-1850851, CCF-2028481. We thank Kurt Wilson and Sudharsan Vaidhun’s contributions to the raw footage.

TABLE I: Comparison of Existing Traffic Sign Datasets.

Dataset	Images	Image Resolution	Classes	Tasks*	Features	Country	Year
STS [3]	3,777	1280×960	20	Both	w/ general occlusion	Sweden	2011
GTSRB [4]	51,839	15×15 ~ 250×250	43	Recognition	w/ general occlusion	Germany	2011
GTSDb [5]	900	1360×1024	43	Detection	w/ general occlusion	Germany	2013
LISA [6]	6,610	640×680 ~ 1024×522	49	Both	w/ general occlusion	USA	2012
TT-100K [7]	100,000 [†]	2048×2048	221	Both	w/ general occlusion	China	2016
MTSD [8]	100,000	1000×1000 ~ 2048×2048	313	Both	w/ general occlusion	Worldwide	2019
DFG [9] [‡]	6,957	720 × 576 ~ 1920×1080	200	Both	w/ general occlusion	Slovenia	2019
GLARE	2,157	720×480~ 1920×1080	41	Both	w/ heavy glares	USA	2022

*We target detection and the recognition (classification) tasks here.

[†]Only 10,000 images contain traffic signs.

[‡]The DFG Traffic Sign Dataset uses polygon annotations, instead of bounding box annotations.

Organization. The rest of the paper is organized as follows: Section II summarizes the existing related work of traffic sign datasets and the cutting-edge object detection models. Section III details the dataset including its collection, annotation, and statistics. Section IV reports the experiments to check the testing performance of the mainstream traffic sign detection algorithms with and without GLARE in the training phase. Section V concludes the paper.¹

II. RELATED WORK

A. Traffic Sign datasets

With the advancement of autonomous driving, there has been an emphasis on collecting data with all types of road conditions, signs, and any factor to note while driving, leading to a plethora of datasets in the community specific to traffic sign detection.

Several datasets tend to focus on traffic signs found globally, each with variations. For example, the German Traffic Sign Recognition Benchmark [5] focuses on traffic signs from Germany and captured images in different environments under varied weather conditions. Others that follow a similar pattern include the Tsinghua-Tencent 100K dataset [7], the Swedish Traffic Sign dataset [3], and the Belgium Traffic Signs dataset [10]. It is advantageous to the computer vision community to have access to traffic signs from around the world, but there is a significant drawback common to public traffic sign datasets: a lack of sun glare within its images.

The use of convolutional neural networks (CNNs) is prevalent throughout traffic sign datasets, often for the tasks of detection and recognition. To set the standard for these tasks, baselines are often attached to datasets in the form of varied CNNs. The Mapillary dataset [8], for example, uses a Faster regional-based convolutional neural network (R-CNN) based detector to produce mean average precision (mAP) results over all of its classes. The DFG Traffic Sign dataset [9] is another example that uses such techniques to establish a baseline, utilizing a Faster R-CNN and a Mask R-CNN to provide mAP values range in the upper 90's. Although the dataset includes traffic-sign instances with synthetic distortions that may resemble sun glare, these images are incomparable to those

with natural sun glare. Because the generalization performance may suffer from improper training with datasets that lack natural sun glare. This is a phenomenon found often throughout datasets focused on traffic sign depiction: models are trained on data without obscuring conditions or with synthetic ones, such as sun glare, usually are unsatisfactory when tested in real driving scenarios.

Severe conditions, such as sun glare or heavy rain, impede the visibility of traffic signs while driving. Just as it hinders human drivers, it additionally interferes with algorithmic vision. The CURE-TSD-Real dataset [11], comprised of traffic sign images in simulated heavy road conditions, is an example of a dataset with severe conditions which resulted in a 29% drop in average precision. This motivates us to investigate the possibility for harsh sun glare to cause a drop in algorithmic performance as well.

GLARE dataset intends to be an extension of the LISA dataset [6], which is one of the most commonly used American traffic sign datasets with an emphasis on large variations within urban landscapes. The dataset is comprised of videos and stand-alone images of traffic signs, amounting to about 6,610 images and 7,855 annotations. Source data for the LISA dataset comes with color, in grayscale, and does not include images with excessive sun glare. The LISA dataset answered a need for a public dataset with US-based traffic signs and notably contributed more as it includes full traceability of its dataset by providing full annotations of all images, and includes all associated tracks. We provide full comparisons of the existing related traffic sign datasets in Table I with GLARE, which shows that GLARE is the latest traffic dataset (with two years gap from DFG and MTSD and nine years gap from original LISA) and it is formed by high-resolution images with heavy/harsh glares on traffic signs.

B. Traffic Sign Classification

One of the most popular applications with the aforementioned datasets is traffic sign classification, where tremendous efforts are accomplished from statistical learning to deep learning paradigm. For example, Soendoro and Supriana [12] firstly adopts the SVMs with the sparse representation to recognize the class of traffic sign in images. With the rise the deep learning, convolutional neural networks begin to dominate

¹GLARE is available at https://github.com/NicholasCG/GLARE_Dataset.

the performances of recognition/classification in the traffic sign domain. Specifically, on the GTSRB dataset, a large amount of CNN variants [13] shows a powerful ability for generalization, where the classification accuracy on the testing set is even better than the performance of human experts (e.g., CNNs with spatial transformers [14] can achieve roughly 99.7% in terms of top-1 accuracy). Note that, the reported high classification accuracy is based on the cropped traffic sign images, where we can obtain these images via a specifically designed detection task.

C. End-to-End Traffic Sign Detection

At first, the detection and the classification are two independent tasks, where the classification is built upon the proper detected images (i.e., the traffic sign is located and extracted intact). With the rise of the CNNs, the original powerful performance of image classification/recognition [15] rapidly transfers to object detection domain. Furthermore, it has been a consensus that the family of CNNs is capable of detecting a bounding box for specific object while classifying its category simultaneously. The well-known RCNN/fast RCNN [16], [17] first generates potential bounding boxes on the frames and then classifies the object only in these bounding boxes. However, the final performance of detection depends on the performances of multiple stages during the complex pipeline (i.e., pre-processing, classification, and post-processing to re-score the proposed bounding boxes), where the whole process is slow as well. To address the efficiency and complexity issue, [18] proposes the first edition of You Only Look Once (YOLO) series, v1 to v5, and treats the object detection as a single regression task to directly establish the connection among the image pixels, the bounding box coordinates and the labels with probabilities. To further improve the performance, YOLOX [19] is proposed as incorporating the anchor-free manner and several cutting-edge detection techniques (e.g., decoupled head, leading label assignment strategy).

Another branch of detection strategies leverage the popular transformer [20] encoder-decoder architectures by removing the complicated hand-designed components such as non-maximum suppression or anchor generation while optimizing a global loss that is enable unique classifications via bipartite matching. Similar ideas are brought into traditional RCNN architecture that a special Swin Transformer [21] shows a great performance gain when replacing the ResNet50 backbone. Almost all the aforementioned detection algorithms rely on the supervised learning with labeled traffic signs and it is rarely considered that the possible strong noises (e.g., sun glare) in the testing phase may degrade the detection performance.

III. GLARE DATASET

This section presents the GLARE traffic sign dataset, a sun glare focused dataset to assist researchers and developers in building real-time autonomous traffic sign detection and classification system in sun glare conditions. The dataset includes 2157 images and annotations, each containing a single traffic sign annotation. This dataset can be used for classification, detection, concurrent detection and classification.

A. Video Collection and Processing

The initial collection process started with three dashboard cameras recording approximately 38 hours of footage around the Orlando area. Two cameras were forward facing with one filmed at 1920×1080 (1080p) and the other rearward facing one filmed at 720×480 (480p). In total, the cameras filmed 463 initial videos of 40 hours and 25 minutes of footage.

The first step in the video processing was to remove all videos that did not meet the criteria of having both sun glare and traffic signs at the time. This results in 163 videos that contained some amount of sun glare. The second step was to extract the sections of video with sun glare, referred to as *clips*. The clips each contained a continuous presence of sun glare, with about a half second of extra time at the start of each clip to allow for ease of finding the beginning of the sun glare. Since only footage that concurrently contains sun glare and traffic signs matters, any clips that did not contain traffic signs during the follow-up screening section were discarded. Following a similar procedure as the LISA dataset [6], these short videos are referred to as *tracks*. 189 tracks were used in the creation of the GLARE dataset, totaling 18 minutes and 11 seconds of footage. The tracks were organized by their original source video, with 33 original source videos being used in total to produce the GLARE dataset.

B. Annotation Process

The image annotation process was separated into two main steps: bounding box localization of traffic signs, and bounding box approval with cleanup. The first step was completed by two individuals at the same time with a single open-source tool [22] to allow for efficient labeling. The second step was completed after the initial processing of all the images as a quality assurance step by two individuals who worked on labeling and processing the initial bounding boxes in the LISA dataset format [6]. The automatic bounding box tracking algorithms available with the tool were Re3 [23] and CMT (Consensus-based Matching and Tracking of Keypoints for Object Tracking) [24], and we used Re3 for all our annotations due to stable tracking at all sizes. When annotations were saved, each image was exported has a single associated annotation.

Traffic Sign Localization. In the first step, tracks were processed together based on the original source video. Each track would then be played to completion, with the bounding box labeling occurring on the first frame with sun glare that was a multiple of 5. The process would continue with the current bounding box being saved on every subsequent multiple of 5 until the track finished playing or sun glare was no longer on the screen. When labeling traffic signs using the bounding box localization tool, you could automatically choose the classification of the traffic sign to allow for increased efficiency. After the initial labeling, the annotation tool would continue automatically annotating until the current user deemed the automatic annotation to have drifted too far. The annotator would then delete and reapply the bounding box, and continue annotating until all the tracks were processed. For each traffic sign in a track, no more than 30 annotations of that traffic sign would be saved to decrease overexposure of that sign.

Bounding Box Approval and Cleanup. After a track was labeled, the annotations were reviewed and either approved or rejected. Any bounding boxes with background noise that can be removed with manual selection are removed and relabeled. After all tracks and annotations were processed, the video was exported in a single CSV file (similar to the LISA dataset) for further processing, as demonstrated by Figure 1.

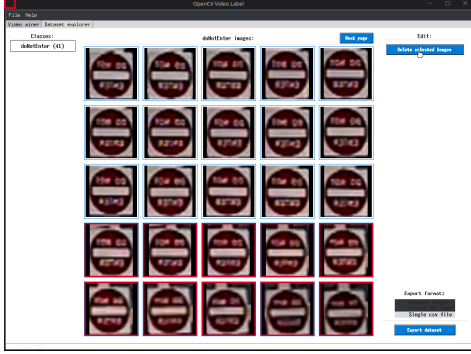


Fig. 1: Bounding box processing and exporting.

After all the tracks were processed and exported by the original source video, the annotations were further processed to remove previously uncaught errors and extract statistical information from the entire dataset. Any bounding box that did not localize a sign or contained significant background noise were rejected, and any improperly labeled annotations were renamed. After removing the improper annotations, the remaining annotations were then categorized on if the traffic signs were covered in any way, and if they were on the current road or a side road [6]. These "Occluded" and "On another road" annotations [6] were then pooled.

C. Dataset Statistics

The GLARE dataset contains 2,157 bounding box annotations and associated images distributed across 41 classes. Figure 2a shows the distributions of the annotations per class. The annotations were created from multiple videos to ensure a variety in the location in glare conditions. For each track in each source video, a maximum of 30 frames for each traffic sign class were allowed to minimize over-exposure of traffic signs in specific positions and sun glare conditions. Figure 2b shows the distribution of annotations across the 33 source videos processed. The size of the bounding box annotations varies between 6×14 and 137×178 pixels, and the size of the images is either 810×540 or 937×540 pixels. The dataset works with existing scripts released alongside the LISA dataset for annotation extraction and splitting [6].

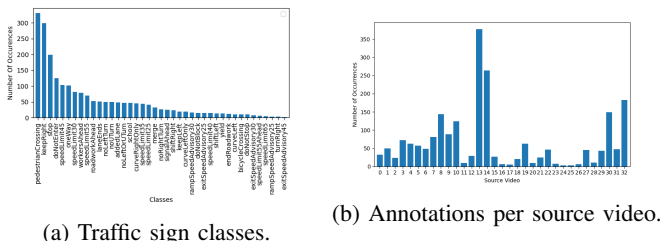


Fig. 2: Statistics/Distributions of GLARE dataset.

The types of visual interference labelled as sun glare can be broadly categorized into four categories. The categories described are subjective, but are recorded to allow for greater understanding on how we evaluated sun glare during the initial video processing for the dataset. Examples of each of the following categories can be seen in Figure 3. The first category is where there is a clear sun without any significant additional bright cloud noise or brightness interference from the camera. The sun appears as a bright ball, excluding any obstruction by either clouds or other objects. In an upcoming section, we will describe a naïve detector for this type of sun glare to improve traffic sign detection results. The second category is where there is a visible sun, but there are additional clouds that add to the overall brightness of the image. The third category is where there is minimal to no visible sun due to cloud interference. Although the sun is not visible in the frame, there is still visual interference that causes traffic signs to be less visible than in clear conditions, decreasing detection. The fourth category is sun glare due to other interference. The sun being visible is not a requirement, as there is visual interference due to the camera settings. Either way, the visual interference appears similar to the interference caused by the other types of sun glare. The images themselves have not been labelled based on type of sun glare due to the subjective nature of the categories and that some images can fit into multiple categories.

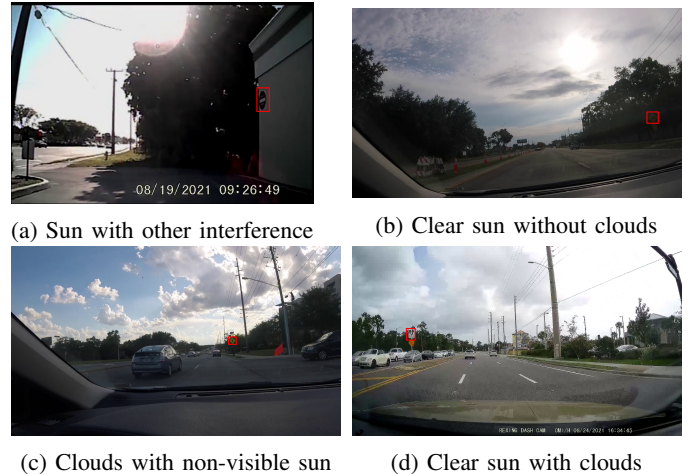


Fig. 3: Examples of images from the GLARE dataset with bounding boxes highlighted.

IV. BENCHMARKS

We tested multiple state of the art methods in detecting traffic signs in sun glare conditions. Each method has two models trained, one on a subset of the GLARE dataset with 80/20 split for training (1725 images) and validation (432 images) and one on the LISA dataset ².

Metrics. The scoring metric used for comparing the performance of the models is the mean average precision (mAP) of the classes as defined in COCO [25] and implemented in

²For the models trained on LISA, the training set is the entire LISA dataset (7855 images), and the validation set is the subset of the GLARE dataset that have classes within the set of classes of the LISA dataset (1725 images).

Ultralytics’ YOLOv5 [26] and OpenMMLab [27]. For each image, we produce multiple predicted bounding boxes, and compare the intersection of each bounding box to the ground truth of the traffic sign in the image. If the predicted bounding box’s Intersection over Union (IoU) with the ground truth is over 0.5, then the prediction is counted as positive. In the case of multiple prediction to a ground truth bounding box, only the prediction with the highest IoU is counted. The Average Precision (AP) is then calculated as the area under the precision-recall curve, and over all classes, we calculate $mAP_{0.5}$ as the mean over all classes with an IoU of 0.5 and $mAP_{0.5:0.95}$ as the mean over all the classes over a range between 0.5 to 0.95, with a step of 0.05 [25].

A. Configured Methods

In order to demonstrate the necessity of viability of the GLARE dataset, we experimented six state-of-the-art methods with detailed **fine-tuned** hyper-parameter settings as follows:

- **Faster-RCNN** [28] and **ResNet50** [29] backbone: We used batch size 2 with a model pretrained on the COCO as the initial weights, and trained for 12 epochs and an initial learning rate of 2.5×10^{-3} with a step decay by 10 after the 8th and 11th epochs.
- **Faster-RCNN** with **Swin Transformer** [21] backbone: We trained with batch size 1 for GLARE and 4 for LISA over 20 epochs. The learning rate was 1×10^{-4} with an AdamW optimizer and decayed over a cosine annealing scheduler with a minimum learning rate of 1×10^{-7} . The learning rate had a linear 10 warmup epochs with a warmup ratio of 0.1.
- **YOLOv5** [26]: We trained for 300 epochs using the small model, as our dataset is meant for real-time application, with LISA model stopping training after 150 epochs due to no improvement, and used a batch size of 64. For the learning rate, we trained with an initial learning rate of 1×10^{-2} with 5 warmup epochs with a linear decay over all epochs.
- **YOLOX**: We trained using the small model for consistency with YOLOv5, and trained for 300 epochs with a batch size of 8 and SGD with Nestrov acceleration. We trained with an initial learning rate of 1.25×10^{-3} with a cosine annealing decay over 250 epochs for the GLARE dataset and 285 epochs for LISA with a final learning rate of 6.25×10^{-5} . The learning rate had an exponential warmup with 5 warmup epochs with a warmup ratio of 1.
- **Deformable DETR** [30]: We trained with a batch size of 2 with an AdamW optimizer for 100 epochs and a gradient clipping norm of 0.1. The initial learning rate was 2×10^{-4} with a step decay by 10 after the 85th epoch for the GLARE dataset and after the 40th epoch for LISA.
- **TOOD** [31]: We trained with a batch size of 2 over 100 epochs for GLARE and 30 epochs for LISA. We trained with an initial learning rate of 1.25×10^{-3} with a step decay after the 16th and 22nd epochs. The learning rate had a linear warmup with 500 warmup iterations and a warmup ratio of 1×10^{-3} .

The YOLOv5 models were trained on Ultralytics’ own testing platform, and the rest of the architectures were trained and validated using OpenMMLab’s MMDetection toolbox [27].

All architectures used the given training and testing pipelines for images so as to not bias the detection results to either dataset. Unless stated otherwise, the initial weights during training were random and training was performed using Stochastic Gradient Descent (SGD). The only alteration from the initial given parameters was the number of epochs and learning rate configurations so as to ensure the convergence of each model. All of the architectures were trained on a single GPU.

B. Experimental Results

The results of testing the GLARE dataset against baseline models trained on the dataset versus trained on the LISA dataset are shown in Table II³.

TABLE II: Detection results of trained architectures when tested on the GLARE dataset

	$mAP_{0.5}$		$mAP_{0.5:0.95}$	
	GLARE	LISA	GLARE	LISA
Faster-RCNN _{ResNet50}	86.00	32.10	58.46	16.41
Faster-RCNN _{SwinT-Base}	90.80	43.80	60.26	20.39
YOLOv5	87.40	20.90	60.70	11.10
YOLOX	89.60	17.70	60.90	9.84
Deformable DETR	87.30	37.70	52.77	18.20
TOOD	88.20	43.60	58.63	20.75

For the models trained on our dataset, the average mAP is 88.22 for IoU = 0.5 and 58.62 for IoU = [0.5, 0.95]. For the models trained on the LISA dataset, the average mAP is 32.47 for IoU = 0.5 and 16.12 for IoU = [0.5, 0.95]. This represents an average decrease of 55.75 points for $mAP_{0.5}$ and an average decrease of 42.5 points for $mAP_{0.5:0.95}$.

Newer architectures have generally greater performance when trained on GLARE, as can be seen by the 1.4 increase between YOLOv5 and a Faster-RCNN with ResNet50 and a 3.4 increase between YOLOv5 and Faster-RCNN with a Swin Transformer on $mAP_{0.5}$. This behavior mostly carries over to $mAP_{0.5:0.95}$ as well, as all architectures, except the Deformable DETR, performed better than the Faster-RCNN with ResNet50.

For the models trained on LISA, there is less consistency in improvement when tested on GLARE. The best performing models are the Faster-RCNN with a Swin Transformer and the TOOD architectures. Both YOLOv5 and YOLOX have a notable decrease in mAP when compared to the average.

All the architectures performing well when trained on GLARE do poorly on LISA. This indicates that sun glare has a notable effect on the ability for current architectures to accurately detect traffic signs. Newer architectures perform better in detecting traffic signs generally in both cases, although there is greater variation in results on LISA. Sun glare affects real-time architectures (such as YOLOv5 and YOLOX) more when trained on LISA.

³The architectures are listed by initial release of the associated publication or code itself if no publication is available.

V. CONCLUSION AND FUTURE WORKS

This paper introduces GLARE, a traffic sign dataset with a focus on sun glare and how it affects the recognition of traffic signs in such conditions. The dataset includes 2,157 images with corresponding bounding box annotations of traffic signs across 41 classes from the Orlando area. The GLARE dataset has a specific focus on images with sun glare present, which affects both human drivers and cameras for autonomous driving systems. Our baseline benchmarks have shown that sun glare has a noticeable effect on the ability of current architectures to detect traffic signs.

The GLARE dataset is the beginning of future research on traffic sign detection in naturally noisy conditions and the removal of sun glare as well. We believe this dataset can be used as a testing set for entire sun glare removal using the U-Net architecture [32], as seen in previous work removing sun flares from images [33]. We also believe this dataset can be extended to include traffic signs in other noisy or abnormal conditions, such as rain, fog, and night-time driving. Such an extension could be used to create and train architectures that can detect traffic signs with greater precision in a wider variety of conditions, whether through image restoration or detection and recognition alone.

REFERENCES

- [1] National Highway Traffic Safety Administration U.S. Department of Transportation. Traffic safety facts: Crash stats — sun glare and slick roads are the two most environment-related causing circumstances., 2015.
- [2] Jiang Bian, Abdullah Al Arafat, Haoyi Xiong, Jing Li, Li Li, Hongyang Chen, Jun Wang, Dejing Dou, and Zhishan Guo. Machine learning in real-time internet of things (iot) systems: A survey. *IEEE Internet of Things Journal*, 9(11):8364–8386, 2022.
- [3] Fredrik Larsson, Michael Felsberg, and P-E Forssen. Correlating fourier descriptors of local patches for road sign recognition. *IET Computer Vision*, 5(4):244–254, 2011.
- [4] Johannes Stallkamp, Marc Schlipsing, Jan Salmen, and Christian Igel. Man vs. computer: Benchmarking machine learning algorithms for traffic sign recognition. *Neural networks*, 32:323–332, 2012.
- [5] Sebastian Houben, Johannes Stallkamp, Jan Salmen, Marc Schlipsing, and Christian Igel. Detection of traffic signs in real-world images: The german traffic sign detection benchmark. In *The 2013 international joint conference on neural networks (IJCNN)*, pages 1–8. Ieee, 2013.
- [6] Andreas Mogelmose, Mohan Manubhai Trivedi, and Thomas B Moeslund. Vision-based traffic sign detection and analysis for intelligent driver assistance systems: Perspectives and survey. *IEEE Transactions on Intelligent Transportation Systems*, 13(4):1484–1497, 2012.
- [7] Zhe Zhu, Dun Liang, Songhai Zhang, Xiaolei Huang, Baoli Li, and Shimin Hu. Traffic-sign detection and classification in the wild. In *Proceedings of the IEEE conference on computer vision and pattern recognition*, pages 2110–2118, 2016.
- [8] Christian Ertler, Jerneja Mislje, Tobias Ollmann, Lorenzo Porzi, Gerhard Neuhold, and Yubin Kuang. The mapillary traffic sign dataset for detection and classification on a global scale. In *European Conference on Computer Vision*, pages 68–84. Springer, 2020.
- [9] Domen Tabernik and Danijel Skočaj. Deep learning for large-scale traffic-sign detection and recognition. *IEEE transactions on intelligent transportation systems*, 21(4):1427–1440, 2019.
- [10] Radu Timofte, Karel Zimmermann, and Luc Van Gool. Multi-view traffic sign detection, recognition, and 3d localisation. *Machine vision and applications*, 25(3):633–647, 2014.
- [11] Dogancan Temel, Min-Hung Chen, and Ghassan AlRegib. Traffic sign detection under challenging conditions: A deeper look into performance variations and spectral characteristics. *IEEE Transactions on Intelligent Transportation Systems*, 21(9):3663–3673, 2019.
- [12] David Soendoro and Iping Supriana. Traffic sign recognition with color-based method, shape-arc estimation and svm. In *Proceedings of the 2011 International Conference on Electrical Engineering and Informatics*, pages 1–6. IEEE, 2011.
- [13] Xuehong Mao, Samer Hijazi, Raúl Casas, Piyush Kaul, Rishi Kumar, and Chris Rowen. Hierarchical cnn for traffic sign recognition. In *2016 IEEE intelligent vehicles symposium (IV)*, pages 130–135. IEEE, 2016.
- [14] Álvaro Arcos-García, Juan A Alvarez-García, and Luis M Soria-Morillo. Deep neural network for traffic sign recognition systems: An analysis of spatial transformers and stochastic optimisation methods. *Neural Networks*, 99:158–165, 2018.
- [15] Alex Krizhevsky, Ilya Sutskever, and Geoffrey E Hinton. Imagenet classification with deep convolutional neural networks. *Advances in neural information processing systems*, 25, 2012.
- [16] Ross Girshick, Jeff Donahue, Trevor Darrell, and Jitendra Malik. Rich feature hierarchies for accurate object detection and semantic segmentation. In *Proceedings of the IEEE conference on computer vision and pattern recognition*, pages 580–587, 2014.
- [17] Ross Girshick. Fast r-cnn. In *Proceedings of the IEEE international conference on computer vision*, pages 1440–1448, 2015.
- [18] Joseph Redmon, Santosh Divvala, Ross Girshick, and Ali Farhadi. You only look once: Unified, real-time object detection. In *Proceedings of the IEEE conference on computer vision and pattern recognition*, pages 779–788, 2016.
- [19] Zheng Ge, Songtao Liu, Feng Wang, Zeming Li, and Jian Sun. YoloX: Exceeding yolo series in 2021. *arXiv preprint arXiv:2107.08430*, 2021.
- [20] Nicolas Carion, Francisco Massa, Gabriel Synnaeve, Nicolas Usunier, Alexander Kirillov, and Sergey Zagoruyko. End-to-end object detection with transformers. In *European conference on computer vision*, pages 213–229. Springer, 2020.
- [21] Ze Liu, Yutong Lin, Yue Cao, Han Hu, Yixuan Wei, Zheng Zhang, Stephen Lin, and Baining Guo. Swin transformer: Hierarchical vision transformer using shifted windows. In *Proceedings of the IEEE/CVF International Conference on Computer Vision*, pages 10012–10022, 2021.
- [22] Nathan de Bruijn. <https://github.com/natdebru/opencv-video-label>, 2019.
- [23] Daniel Gordon, Ali Farhadi, and Dieter Fox. Re3: Real-time recurrent regression networks for visual tracking of generic objects. *IEEE Robotics and Automation Letters*, 3(2):788–795, 2018.
- [24] Georg Nebel and Roman Pflugfelder. Clustering of Static-Adaptive correspondences for deformable object tracking. In *Computer Vision and Pattern Recognition*. IEEE, June 2015.
- [25] Tsung-Yi Lin, Michael Maire, Serge Belongie, James Hays, Pietro Perona, Deva Ramanan, Piotr Dollar, and Larry Zitnick. Microsoft coco: Common objects in context. In *ECCV. European Conference on Computer Vision*, September 2014.
- [26] Glenn Jocher, Ayush Chaurasia, Alex Stoken, Jirka Borovec, NanoCode012, Yonghye Kwon, TaoXie, Jiacong Fang, imyhxy, Kalen Michael, Lorna, Abhiram V, Diego Montes, Jebastin Nadar, Laughing, tkianai, yxNONG, Piotr Skalski, Zhiqiang Wang, Adam Hogan, Cristi Fati, Lorenzo Mammama, AlexWang1900, Deep Patel, Ding Yiwei, Felix You, Jan Hajek, Laurentiu Diaconu, and Mai Thanh Minh. ultralytics/yolov5: v6.1 - TensorRT, TensorFlow Edge TPU and OpenVINO Export and Inference, February 2022.
- [27] Kai Chen, Jiaqi Wang, Jiangmiao Pang, Yuhang Cao, Yu Xiong, Xiaoxiao Li, Shuyang Sun, Wansen Feng, Ziwei Liu, Jiarui Xu, Zheng Zhang, Dazhi Cheng, Chenchen Zhu, Tianheng Cheng, Qijie Zhao, Buyu Li, Xin Lu, Rui Zhu, Yue Wu, Jifeng Dai, Jingdong Wang, Jianping Shi, Wanli Ouyang, Chen Change Loy, and Dahua Lin. MMDetection: Open mmlab detection toolbox and benchmark. *arXiv preprint arXiv:1906.07155*, 2019.
- [28] Shaoqing Ren, Kaiming He, Ross Girshick, and Jian Sun. Faster r-cnn: Towards real-time object detection with region proposal networks. *IEEE Transactions on Pattern Analysis and Machine Intelligence*, Jun 2017.
- [29] Kaiming He, Xiangyu Zhang, Shaoqing Ren, and Jian Sun. Deep residual learning for image recognition, 2015.
- [30] Xizhou Zhu, Weijie Su, Lewei Lu, Bin Li, Xiaogang Wang, and Jifeng Dai. Deformable detr: Deformable transformers for end-to-end object detection. In *International Conference on Learning Representations*, 2021.
- [31] Chengjian Feng, Yujie Zhong, Yu Gao, Matthew R Scott, and Weilin Huang. Tood: Task-aligned one-stage object detection. In *ICCV*, 2021.
- [32] Olaf Ronneberger, Philipp Fischer, and Thomas Brox. U-net: Convolutional networks for biomedical image segmentation, 2015.
- [33] Yicheng Wu, Qirui He, Tianfan Xue, Rahul Garg, Jiawen Chen, Ashok Veeraraghavan, and Jonathan T. Barron. How to train neural networks for flare removal, 2020.